Metal-insulator transition in a doped semiconductor

T. F. Rosenbaum,* R. F. Milligan,† M. A. Paalanen, G. A. Thomas, and R. N. Bhatt
Bell Laboratories, Murray Hill, New Jersey 07974

W. Lin
Bell Laboratories, Allentown, Pennsylvania 18104

(Received 3 December 1982)

Millikelvin measurements of the conductivity as a function of donor density and uniaxial stress in bulk samples of phosphorus-doped silicon establish that the transition from metal to insulator is continuous, but sharper than predicted by scaling theories of localization. The divergence of the dielectric susceptibility as the transition is approached from below also points out problems in current scaling theories. The temperature dependence of the conductivity and the magnetoresistance in the metal indicate the importance of Coulomb interactions in describing the behavior of disordered systems.

I. INTRODUCTION

Doped semiconductors have been widely studied to probe the nature of the metal-insulator transition in disordered systems.[1,2] Si:P is a well-characterized, homogeneous system where P donors sit substitutionally and randomly in a dislocation-free Si lattice. The outer electron of the shallow donor moves with a large effective Bohr radius a_B which encompasses many lattice sites. This makes the discreteness of the lattice unimportant in describing the interaction between neighboring donors. In Si:P, a_B is ~ 17 Å while the nearest-neighbor distance of the Si lattice is 2.35 Å. At low donor concentrations (n) there is negligible overlap of the hydrogenic wave functions of these donor electrons, and the material is an insulator at temperature $T=0$. At high concentrations when the overlap is large compared to the on-site electron-electron repulsion, the material is a metal. The transition from the insulating to metallic state (i.e., localized to itinerant electrons) occurs at a critical concentration n_c, when the average spacing between the impurities, $n_c^{-1/3}$, is about 4 times the Bohr radius as observed in a variety of materials with greatly different values of n_c. This led Mott[1] to the following universal scaling form:

$$n_c^{1/3} a_B \simeq 0.25 \tag{1}$$

which is confirmed by data in systems with n_c varying over 9 orders of magnitude.

Another view of the transition, due to Anderson,[3] involves localization due to random one-electron potentials seen by the electrons. For low donor concentrations the energy spread in the random potentials of the disordered system is large compared to the energy bandwidth and the electronic states of the system are localized. At higher concentrations, extended states appear, separated in energy from the localized states by a mobility edge E_c. Within this framework,[4] the metal-insulator transition occurs when the addition of electrons pushes the Fermi level E_F through E_c from the localized to the extended side at n_c.[1]

Competing theories have recently been proposed to describe the specific features of disordered systems near the metal-insulator transition. Scaling theories of localization[5,6] suggest that the zero-temperature electrical conductivity $\sigma(0)$ decreases continuously as n is lowered to n_c. A corresponding critical divergence is predicted in the dielectric constant as n is raised to n_c on the insulating side. In contrast, Mott[7] has proposed that $\sigma(0)$ decreases continuously with n only until a minimum value of conductivity σ_M is reached. Reducing n further causes $\sigma(0)$ to drop discontinuously to zero. Mott's reasoning is based on the Ioffe-Regel[8] criterion (that in a metallic state, the electronic mean free path cannot be less than the interdonor spacing), plus considerations of Anderson localization.[7]

Recently, the contribution of both Coulomb interactions[9–12] and localization[13–15] effects to the low-T transport properties of disordered, metallic systems have been calculated. The temperature corrections to $\sigma(0)$, as well as magnetic field effects (magnetoresistance and Hall effect), have been considered. Models in which the electronic transport proceeds by hopping have also considered the effects of finite T,[2,16,17] electric field,[16,17] and magnetic field.[18,19]

Experimental measurements of transport proper-

ties of Si:P have a long history. Alexander and Holcomb[20] and Fritzsche[21] have written excellent reviews of the early work and more recent work, respectively. The experiments which are of concern to us in this paper are those taken at very low T ($T<1$ K) for samples close to the transition. It is in this regime where the measured transport properties distinguish between competing theories.

The temperature correction to $\sigma(0)$ for just metallic samples has been found[22] to vary as $T^{1/2}$ at low temperatures while the sign of the correction depends on n. These results are in quantitative agreement with the Coulomb interaction model when effects of many valleys, mass anisotropy, and intervalley scattering are taken into account.[12] Recent measurements[23] on Ge:Sb yield similar results, although the square-root dependence is restricted to a smaller temperature range than is found for the Si:P case. Analyzing the Ge:Sb data to higher temperatures requires the addition of a term linear in T which might be due to inelastic electron-electron scattering, a localization effect. The variation of $\sigma(0)$ with n has been measured for a series of uncompensated Si:P samples.[24] The transition is extremely sharp and fits a scaling form for $2\sigma_M \lesssim \sigma(0) < 13\sigma_M$. Measurements on Si:P samples under uniaxial stress[25] have shown that samples which are just localized at zero stress can be stress tuned through the transition. $\sigma(0)$ vs n/n_c thus obtained agrees with the zero-stress results and extends the fit to the scaling form to $\sim\frac{1}{4}\sigma_M$ or $(n-n_c)/n_c \sim 10^{-3}$. Although the variation of $\sigma(0)$ fits a power law in $n-n_c$ as predicted by the scaling theory, the exponent is quite different, and the prefactor an order of magnitude larger; thus the transition is sharper than predicted. Measurements on Ge:Sb (Ref. 26) samples with small amounts of compensation exhibited a rapid decrease of $\sigma(0)$ as n was reduced to n_c similar to Si:P. Samples with larger compensation behaved in a manner which increasingly approached that predicted by the scaling theory of localization,[5] prompting the suggestion[26] that the rapid n dependence of the uncompensated Si:P sample is due to Coulomb interaction effects. In the Anderson localization model $\sigma(0)$ is zero for $n<n_c$ even though the electron density of states remains finite. Specific-heat measurements[27] on a series of Si:P samples have shown that the density of states for electron-hole excitations does remain finite through the transition.

Recent measurements[28] of the magnetoresistance of barely metallic Si:P samples below 100 mK have found contributions from both the localization[15] and Coulomb interaction[12] models. The positive magnetoresistance, arising from the Coulomb interactions, dominates near the transition. The negative magnetoresistance, which is observed in more metallic samples at low fields, is thought to be due to localization effects. Both effects have a square-root field (H) dependence at sufficiently large H. Low-temperature magnetoresistance measurements on metallic Ge:Sb by Ootuka *et al.*[29] show a similar square-root dependence which we have interpreted[28] in the same manner as the Si:P data.

On the insulating side of the transition, the electronic conduction[30] seems to proceed by electrons hopping[16,17] from one localized state to a neighboring state. The characteristic length obtained[30] from the data using these models is, however, unexpectedly large. Measurements of donor spin susceptibility[31] can be analyzed quantitatively[32] in terms of localized electrons interacting via Heisenberg antiferromagnetic exchange for $n<n_c$. At low temperatures the susceptibility rapidly drops as n is raised through the transition, indicating a change from localized electronic states to nearly degenerate states.

The low-frequency dielectric susceptibility χ has been measured directly[33,34] and calculated from optical data[35,36] for samples just below the transition. The divergence of χ can be analyzed[24,36] in terms of a diverging localization length which is the counterpart to the length which enters $\sigma(0)$ as n approaches n_c from the metallic side.

Many workers have measured the infrared-absorption spectra of Si:P as a function of donor concentration.[1,2,37] At low concentrations ($n<2\times10^{17}$ cm^{-3}) the spectra of individual donors are prominent. As n increases, donor pairs appear, and the spectrum becomes nearly featureless as relatively large, random clusters dominate the absorption for $0.2\times10^{18}<n<4\times10^{18}$. The data can be explained assuming a random distribution of donor sites.[37]

II. EXPERIMENTAL DETAILS

Low-T, four-probe electrical measurements were made using commerical quality Czochralski-grown Si:P crystals. After cutting the samples to the appropriate size the surfaces were etched to remove the damaged surface layer. Ootuka and co-workers[38] have shown that this layer leads to significant surface conduction. Wires of Au:Sn were spot welded to the freshly etched surfaces to make contacts whose resistances were less than 1% of that of the sample. The contacts were arranged linearly with an average length between voltage probes of 1 mm along an average cross-sectional area of 0.8×0.5 mm^2. Current flow homogeneity was tested by unnesting the voltage and current leads and observing the check voltages; these voltages were noise-limited and less than 10^{-3} of the nested voltage.[39] Voltages were measured using phase sensitive detection at low

frequency (~ 10 Hz) and were independent of frequency to at least 1 kHz. Power input to the sample was in the range of 10^{-17}–10^{-12} W. No measurable heating of the crystal lattice was observed, although certain samples exhibited an electric-field-dependent conductivity, as discussed in Sec. III D. Temperatures down to 1 mK were achieved[40] by dilution refrigerators with adiabatic demagnetization of Cu or $PrNi_5$. Samples and thermometers were attached to a silver bar with a thin layer of Apiezon grease and were thermally sunk primarily via the leads.

Donor concentrations n were determined by measuring the room T resistivities of samples and using the calibration of Mousty *et al.*[41] based on neutron activation analysis. The resistivity ratio $\rho(4.2\text{ K})/\rho(293\text{ K})$ allows a more accurate determination of relative concentrations.[30]

III. EXPERIMENTAL RESULTS

A. An overview

Figure 1 shows the resistivity ρ of four different samples of Si:P plotted over more than 4 orders of magnitude of temperature. The sample with donor concentration $\tilde{n} \equiv n/10^{18}\text{ cm}^{-3} = 7.0$ clearly behaves like a metal at low temperature, i.e., ρ decreases with decreasing T and is finite at $T=0$. The sample with $\tilde{n}=3.84$ is insulatorlike in its T dependence with an extrapolated zero T conductivity $\sigma(0)$ above Mott's minimum metallic conductivity[7] $\sigma_M = 0.05e^2/\hbar d_c$. Here d_c is the average spacing between impurity atoms of concentration n_c at the metal-insulator transition. Using $d_c = (n_c)^{-1/3}$ gives $\sigma_M = 20\ (\Omega\text{ cm})^{-1}$ ($1/\sigma_M = 0.05\ \Omega$ cm is shown by the arrow in Fig. 1). The sample with $\tilde{n}=3.75$ is very close to the transition and is insulatorlike in its temperature dependence with $\sigma(0) < \sigma_M$. This sample is a metal by our definition because it has finite σ in the limit $T \to 0$ K. The $\tilde{n}=3.70$ sample is on the insulating side of the transition since ρ increases exponentially with decreasing T and thus becomes infinite as $T \to 0$ K. The sensitivity of the low temperature ρ to small changes in impurity concentration for samples near n_c is clearly seen in this figure. The three samples near n_c have concentrations which differ by $\sim 4\%$ with nearly identical values of ρ at room temperature. However, at 4.2 K the value of ρ for the $\tilde{n}=3.7$ sample is nearly an order of magnitude greater than that for the $\tilde{n}=3.84$ sample. We have characterized the samples by measuring the ratio $\rho(4.2\text{ K})/\rho(293\text{ K})$ as mentioned previously.[30] Samples with a resistivity ratio near 5 are very close to the transition.

Figure 2 shows the effect of donor concentration

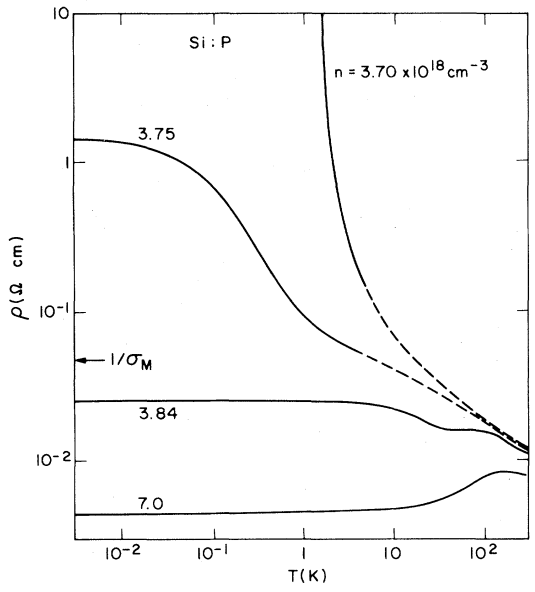

FIG. 1. Resistivity ρ vs temperature T for several samples of Si:P with donor density n above and below the critical density $n_c = 3.74 \times 10^{18}$ cm^{-3}. Near n_c a small change in n has a large effect on $\rho(T)$.

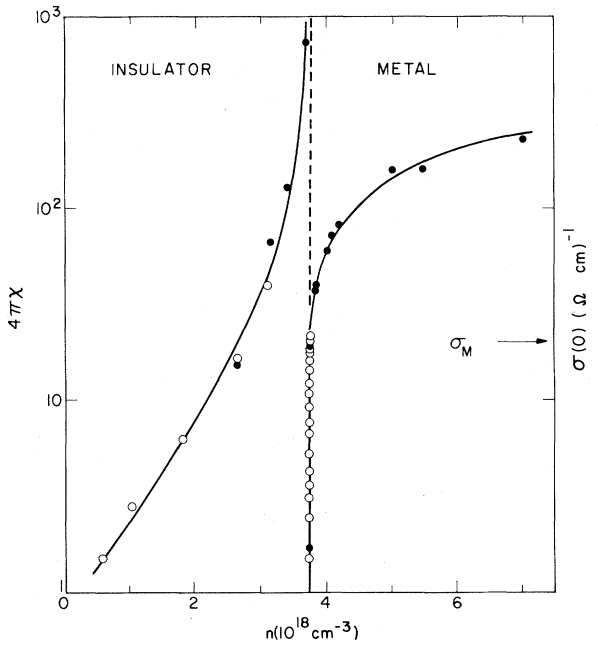

FIG. 2. Divergence of the $T=0$ K donor dielectric susceptibility $4\pi\chi$ in the insulator [open circles, Ref. 34; solid circles, Ref. 32; solid line, Eq. (6)] and the $T=0$ K conductivity $\sigma(0)$ in the metal [solid circles, Ref. 36; open circles, Ref. 24; solid line, Eq. (4)] as a function of phosphorus donor density n. Together these results characterize the metal-insulator transition in a disordered system.

on the low-T values of the two physical quantities which characterize the metal-insulator transition: $\sigma(0)$ and χ. The plots of $\sigma(0)$ and χ in Fig. 2 are highly suggestive of critical behavior. The sharpness of this transition is remarkable and is close qualitatively to the discontinuity predicted by Mott.[7] Scaling theories of localization[5] predict an expression for $\sigma(0)$ which can be written

$$\sigma(0)=C_L e^2/\hbar\xi\ , \tag{2}$$

where C_L is a constant and ξ is the scale length which near n_c has the critical form

$$\xi=\xi_0[(n/n_c)-1]^{-\nu}\ . \tag{3}$$

As a function of n, $\sigma(0)$ becomes

$$\sigma(0)=\sigma_c[(n/n_c)-1]^{\nu}\ . \tag{4}$$

The scaling models are estimated to be applicable for $\sigma(0)<\sigma_M$ or $|n/n_c-1|\lesssim 1\%$ so values of n/n_c of this precision are required to test the critical behavior. Empirically, we have argued that critical behavior appears to occur over a wider range, i.e., $\sigma(0)\lesssim\sigma_{\rm IR}$, where $\sigma_{\rm IR}$ is the Ioffe-Regel conductivity at which $k_F l\sim 2$. For Si:P, $\sigma_{\rm IR}\approx 10\sigma_M$ and at that point $n/n_c\sim 2$. For $n/n_c-1>3\%$, we can determine n accurately enough to analyze the data from our series of samples quantitatively. In the Appendix we show that the calculated Boltzmann conductivity differs substantially from our measured $\sigma(0)$ over the large region up to $n/n_c\sim 2$. Using the range $1.03<n/n_c<2$, we find that the data fit the form of Eq. (4) with $\sigma_0=260\pm 30$ $(\Omega\,{\rm cm})^{-1}$ and $\nu=0.55\pm 0.1$.

The relatively slow variation of $\rho(293\ {\rm K})$ with n, and uncertainties in sample size, combine to give an absolute error of $\pm 5\%$ in n. We have determined relative concentrations n/n_c to about 1% accuracy using the resistivity ratios, which vary rapidly near n_c.[28] In addition to uncertainties in average donor concentration, there is the question of sample inhomogeneity on a scale much larger than ξ. Our contactless and movable probe measurements have shown variations in n of only $\sim 0.04\%$ over a scale of ~ 1 mm. The reproducibility and consistency that we have observed in our stress studies shows that either the nonrandom inhomogeneities on the scale between 1 mm and ξ are insignificant or that they enter in a surprisingly similar way in different samples.

The filled circles for $\sigma(0)$ shown in Fig. 2 are from samples with different values of n. An alternate approach to studying the transition is to start with a single barely localized sample and change n_c by applying uniaxial stress. Application of stress mixes extended excited state wave functions with the ground state thereby increasing a_B. This reduces n_c as shown by Eq. (1). Such stress tuning through the transition has recently been reported[25] and the open circles in Fig. 2 are from the stress results.

In that paper we show that over a narrow range, n_c is nearly linear with the stress s. In Fig. 3 we plot $\sigma(s)$ at three temperatures to illustrate the importance of measurements in the millikelvin regime. Considering Eq. (4), we have extrapolated[25] our results to $T=0$ K and have tested for critical behavior of the form

$$\sigma(0)\propto(s-s_c)^{\nu}\ , \tag{5}$$

where s_c is a critical value of stress which depends on n. Analyzing the data in this fashion has yielded reproducible values of $\sigma(0)$ for n/n_c-1 as low as 10^{-3}. The results for one sample are shown in Fig. 4 versus both uniaxial stress and corresponding density n/n_c-1. For comparison, we plot the predictions of Mott and the scaling theory of localization as dashed lines on the same scale. We find that the critical behavior of $\sigma(0)$ within this region is the same as that in the precursive region, with $\nu=0.48\pm 0.07$. This smooth variation from critical to precursive regions suggests that these two regions are indistinguishable or that the critical region is as large as $n/n_c-1\lesssim 1$ (see also recent theoretical ar-

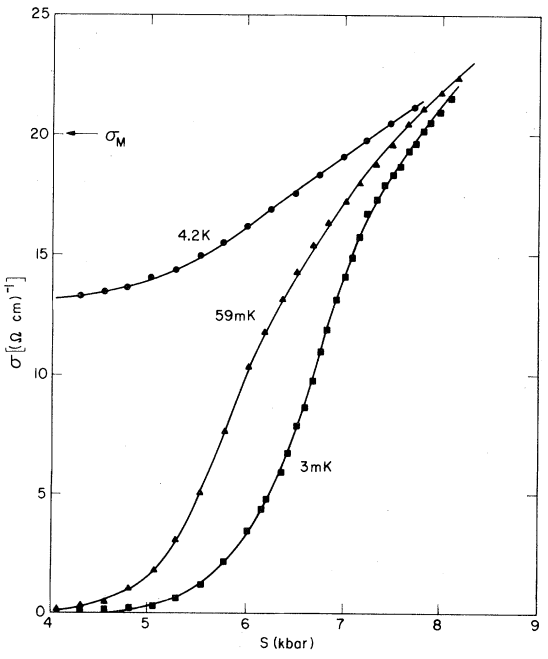

FIG. 3. Conductivity σ as a function of uniaxial stress s at three temperatures for a sample tuned through the metal-insulator transition. Low T is essential for determining the true $T=0$ K behavior.

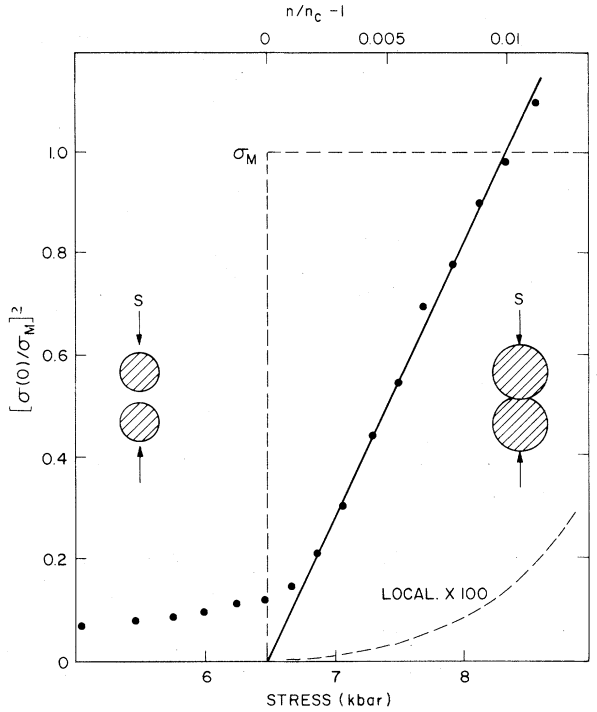

FIG. 4. Extrapolated $T=0$ K values of σ normalized to Mott's minimum metallic conductivity σ_M as a function of uniaxial stress s (bottom scale) and reduced phosphorus density n/n_c-1 (top scale). The solid line gives $\nu=\frac{1}{2}$ in Eq. (4), the dashed lines are Mott's prediction of a discontinuity at σ_M and that of the scaling theory of localization multiplied by a factor of 100.

guments[42]). The tail for $s \lesssim 6.5$ kbar in Fig. 4 is exponential in s but does not reproduce in magnitude.

A similar critical approach to the transition is exhibited by the zero-frequency dielectric constant on the insulating side, as shown in Fig. 2. By a simple dimensional argument we obtain $\chi \propto n\xi_L^2$, where ξ_L is the localization length. Within a metallic region at wave vector q, $\chi=\kappa_s^2/q^2$, where κ_s^{-1} is the Thomas-Fermi screening length. As $q\to 0$ for localized states, $1/q^2$ must be cutoff by ξ_L^2, giving $\chi(q\to 0)=\chi(0)=\kappa_s^2\xi_L^2$. Götze[6] finds $\chi(0)\propto 1/\sigma^2$ at equal values of $|n-n_c|$ so that ζ would be 2ν. Imry[42] also finds $\chi \propto n\xi_L^2$ within a scaling theory approach. Using a scaling theory and quantum diffusion, McMillian[14] finds $\chi \propto \xi^{(\eta-1)}$, where $1<\eta<3$. Within McMillian's formulation, we obtain $\eta=3.3\pm 0.5$ implying that the system is near the limit of no Coulomb interactions where $\eta=3$. However, a variety of measurements on doped semiconductors (see below) suggests that these interactions are strong. McMillan has interpreted the tunneling results[43] in metallic granular Al as indicating a different value of η (~ 2), consistent with strong interactions within his formalism.

The open circles for χ in Fig. 2 were obtained using a Kramers-Kronig transformation of infrared-absorption spectra.[36] The results are in agreement with the far-infrared interference measurements of Townsend[33] and the low-frequency capacitance measurements of Castner *et al.*[33] The latter have emphasized the divergent behavior of χ near n_c. More recent data[34] (filled circles) obtained using a transmission cavity at 400 MHz and temperatures down to 20 mK agree with the infrared results.

In Fig. 5 we summarize our results on the metal-insulator transition by plotting both $\sigma(0)$ and $\chi^{-1/2}$ against density on a logarithmic scale. The data for $\sigma(0)$ fits the form of Eq. (4) with $\sigma_0=260$ $(\Omega\,\mathrm{cm})^{-1}$ and $\nu=0.48\pm 0.07$ while χ fits the form

$$4\pi\chi=\chi_0(n_c/n-1)^{-\zeta}, \tag{6}$$

with $\chi_0=7.0$ and $\zeta=1.15\pm 0.15$.

There are several important features concerning Fig. 5. First, if $\sigma(0)$ and χ are analyzed in terms of a divergent length, this length behaves critically with the same form as n_c is approached from either above or below. Next, the value of $\nu\sim\zeta/2\sim\frac{1}{2}$ differs from that expected from scaling theory[5] (and from results[26] on compensated semiconductors and on a-$Si_{1-x}Nb_x$) ($\nu\simeq 1$), while the prefactor σ_0 is roughly 13 times greater than the predicted value [$\sigma_M\cong 20$ $(\Omega\,\mathrm{cm})^{-1}$]. Finally, we see that there is no

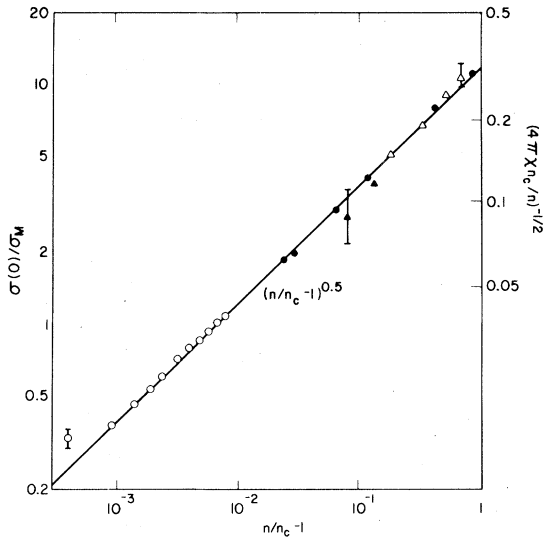

FIG. 5. Data of Fig. 2 plotted on a logarithmic scale to emphasize the symmetry of Eqs. (4) and (6), with $\nu\simeq\zeta/2\simeq 0.5$. The region over which a critical form can be fitted, $n/n_c-1\lesssim 1$, is considerably larger than the conventional expectation of $n/n_c-1\lesssim 0.01$.

indication of a discontinuous drop in $\sigma(0)$ close to the transition. We interpret these results as indicating that the existence of Mott's minimum metallic conductivity for this system is unlikely. The numerical disagreement of ν and σ_0 may be an indication of Coulomb interaction effects. Recent measurements on Ge:Sb (Ref. 26) show that samples with low compensation have $\nu=\frac{1}{2}$ and $\sigma_0>\sigma_M$. As compensation is increased the values of ν and σ_0 approach the localization predictions. One interpretation of these results is that, by increasing the compensation but keeping n constant, the effects of localization are increased while the density of donor electrons, hence interaction effects, remain constant. We also note that a contribution from interaction effects are required to explain the temperature and magnetic field dependence of σ for both Si:P and Ge:Sb, as described below.

B. Temperature dependence of the conductivity

We have found that at low temperature ($T<1$ K) $\sigma(T)$ for our metallic samples can be fit to the form

$$\sigma(T)=\sigma(0)+mT^{\beta} . \tag{7}$$

Figure 6 shows both linear and logarithmic plots of $\sigma(T)$ vs T for a sample with $\sigma(0)=11\sigma_M$. The cusplike approach to $T=0$ indicates $\beta<1$; this shape is characteristic of our samples with $\sigma(0)>\sigma_M$. Averaged over our metallic samples we find $\beta\sim\frac{1}{2}$ for $T<1$ K. The solid lines in Fig. 6 are for $\beta=\frac{1}{2}$ with experimentally determined values of $\sigma(0)$ and m. The cusplike behavior at low T is quite different from that of crystalline metals for which $\beta>1$. (Although the P donors occupy sites in the crystalline Si lattice, their arrangement provides an apparently random potential.[35,36])

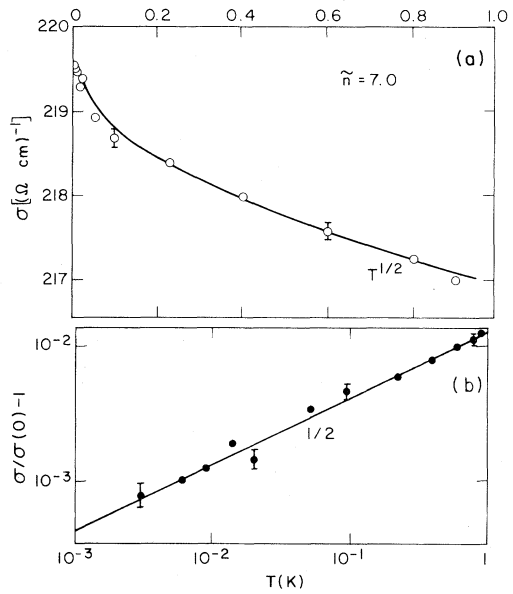

FIG. 6. (a) σ vs T for a sample with $\tilde{n}=7.0$ and $\sigma(0)=11\sigma_M$. $\sigma(0)$ is determined by extrapolating to $T=0$. The solid ine is calculated from Eq. (7) with $\beta=\frac{1}{2}$. (b) Log plot of $\sigma/\sigma(0)-1$ vs T. Solid line has a slope of $\frac{1}{2}$.

For disordered metals there are two approaches to calculate the first-order temperature correction to $\sigma(0)$ [Eq. (7)]. The first model is the zero-T scaling theory of localization extended to include inelastic scattering but neglecting Coulomb interactions.[5,15] This yields a positive correction factor with β determined by the dominant inelastic scattering mechanism. Because the sign of m in this model is opposite to that observed, this contribution must be extremely small. Thomas *et al.*[27] have interpreted similar results in Ge:Sb as indicating a possible contribution of this localization type with electron-electron inelastic scattering.

The second approach, due originally to Altshuler and Aronov[9] and later to others[10–12] predicts an exponent $\beta=\frac{1}{2}$ and a magnitude m which can change sign with donor density. They consider Coulomb interactions with electron-electron scattering in the presence of the random impurities. These calculations are valid for $k_F l\gg 1$.

The following free-electron formulas[44,45] are used in the calculation of $\sigma(T)$: Fermi wave vector

$$k_F=\left[\frac{3\pi^2 n}{v'}\right]^{1/3} , \tag{8}$$

where $v'=6$ for Si and $v'=4$ for Ge. The Fermi energy

$$\epsilon_F=\hbar^2 k_F^2/2m^* , \tag{9}$$

where the effective mass $m^*=0.26m_e$ for Si and $0.11m_e$ for Ge. The Fermi temperature

$$T_F=\epsilon_F/k_B . \tag{10}$$

The mean free path

$$l=\frac{3\pi^2}{4}\frac{\hbar}{e^2}\frac{\sigma(0)}{k_F^2}=\frac{3m^*D}{\hbar k_F} , \tag{11}$$

where D is the diffusion constant. The screening wave vector

$$K=\left[\frac{12\pi n m^* e^2}{\epsilon_0\hbar^2 k_F^2}\right]^{1/2} , \tag{12}$$

where the dielectric constant[33] $\epsilon_0=11.4$ for Si and 15.36 for Ge. In Si only two valleys are effective in the screening process,[12] so k_F that enters[12] K has

$v'=2$.

The theoretical conductivity is given by

$$\sigma(T)=\sigma(0)+\alpha(\tfrac{4}{3}-\lambda F)\sqrt{T}\ , \tag{13}$$

where $\lambda=2$ for a single, isotropic valley, but because of anisotropy factors,[12] $\lambda=4$ for Si:P and $\lambda=12$ for Ge:Sb. For both cases

$$\alpha=\left[T_F\left[\frac{m^*D}{\hbar}\right]\right]^{-1/2}.$$

The dimensionless term F is a function of $\chi\equiv(2k_F/K)^2$ and results from the Hartree interaction. It is given by

$$F=\ln[(1+X)/X]\ , \tag{14}$$

and ranges from 0 to 1. Bhatt and Lee[12] show that Si:P can be described by moderate anisotropy and Ge:Sb by large anisotropy, with negligible intervalley scattering in both, so that

$$X=(n/10^{18})^{1/3}\times\begin{cases}2.3 & \text{for Ge}\\ 0.5 & \text{for Si.}\end{cases} \tag{15}$$

Far above the transition X is large and $F\to 0$. This produces a positive value for m in some systems. Closer to the transition, where most of our data is taken, $X\lesssim 1$ and $\lambda F>\frac{4}{3}$, yielding negative values of m. Near n_c, K may become small[22] and $F\to 0$ again, explaining qualitatively the observed sign change in m.

Figure 7 shows m plotted against n for five samples, where m is found from a least-squares fit to Eq. (7) with $\beta=\frac{1}{2}$. Below $\tilde{n}\simeq 6$, k_Fl is no longer significantly greater than 1, the condition required for the derivation of Eq. (13). Nonetheless, this expression still describes qualitatively the behavior of m. The rapid increase in the value of m as $n\to n_c$ is consistent with Eq. (13). Using Eq. (11) we see that $D\propto\sigma(0)$ which makes α proportional to $\sigma(0)^{-1/2}$. As $n\to n_c$ the precipitous drop in $\sigma(0)$ causes the magnitude of α to increase rapidly. The solid line in Fig. 7 is calculated from Eq. (13) using the measured values of $\sigma(0)$. The line is given by the theory[12] and fits the data without adjustable parameters.

A similar negative $T^{1/2}$ correction to $\sigma(0)$ has been found by Thomas *et al.*[23] for Ge:Sb. Again the sign of the temperature correction becomes positive for n just above $n_c=1.55\times10^{17}$ cm^{-3}. Unlike Si:P, the Ge:Sb system has a very restricted range of T ($\lesssim$170 mK) for which Eq. (5) provides a good fit. This small-T range may be due to the smaller characteristic electronic and lattice energies for Ge compared to Si. Adding a positive term proportional to T to Eq. (7) extends the applicable temperature range to $\sim$0.5 K. The positive T term is based on the scaling theory of localization[13] where the inelastic scattering rate is dominated by electron-electron scattering.

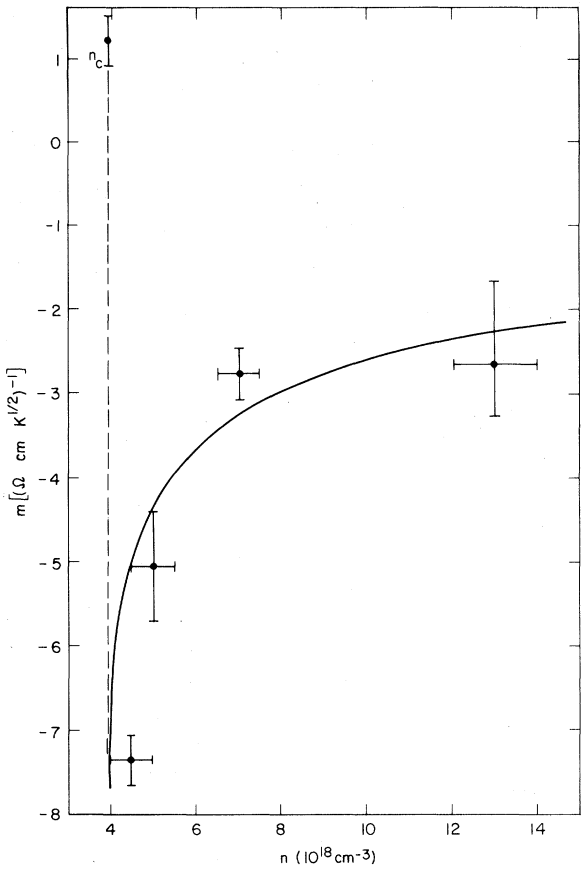

FIG. 7. Factor m from Eq. (7), determined via a least-squares fit with $\beta=\frac{1}{2}$, plotted for several samples. m becomes large and negative as n_c is approached per Eq. (13). Very close to n_c screening breaks down causing m to change sign (the dashed line is a guide to the eye). The solid line is calculated from Eq. (13) multiplied by 6.7.

As with the Si:P case, the magnitude of m for Ge:Sb dramatically increases as $n\to n_c$, in qualitative agreement with Eq. (11). However, at a given value of n the experimental value of m is in good agreement with the theoretical value, if fewer valleys than $\bar{v}$ are included in the screening.[12] The observed temperature correction to $\sigma(0)$ is larger[27] for Ge:Sb than for Si:P, as predicted by Eq. (12) with anisotropy taken into account.[12]

C. Magnetic field dependence of the conductivity

We have seen that there is a temperature correction for $\sigma(0)$ which is positive for the localization

model[14] and of either sign for the Coulomb interaction model.[11,12] Application of a magnetic field H gives $H^{1/2}$ corrections to $\sigma(0)$ which are positive for the localization model[15] and negative (positive magnetoresistance) for the Coulomb interaction model.[12] Magnetic field studies should, therefore, give important clues to the magnitudes of these competing effects.

Lee and Ramakrishnan have shown[11] that for the interaction model in the limit of $m_e D/\hbar \gg 1$ a positive magnetoresistance is produced due to the spin splitting of electrons with opposite spin. The energy splitting is of the usual form, $g\mu_B H$.

In the presence of a magnetic field H, Eq. (13) becomes[12]

$$\sigma(H,T)=\sigma(0,0)+\alpha(\tfrac{4}{3}-F)\sqrt{T} -\alpha F\sqrt{T}\,G(h)/G(0)\ , \tag{16}$$

where

$$G(h)=\int_0^\infty dW\frac{\partial}{\partial W^2} \times\left[\frac{W}{e^W-1}\right](\sqrt{W+h}+\sqrt{|W-h|})$$

and $h=g\mu_B H/kT$. The resistivity $\rho(H,T)=1/\sigma(H,T)$ is easily found from Eq. (16). For small corrections we get

$$\rho(H,T)=\rho(0,0)-\alpha\rho^2(0,0)(\tfrac{4}{3}-F)\sqrt{T} +\alpha\rho^2(0,0)F\sqrt{T}\,G(h)/G(0)\ . \tag{17}$$

At the low temperature of these experiments $h \gg 1$ for H of only a few hundred oersted. In this limit $G(h)/G(0)=0.77\sqrt{h}$. In the low-field limit, $h \ll 1$, $G(h)/G(0)\approx 1+0(h^2)$. Equation (15) shows us that the magnetoresistance is always positive and in the high-field limit we get

$$\rho(H,T)=\rho(0,0)-\alpha\rho^2(0,0)(\tfrac{4}{3}-F)\sqrt{T} +0.77\alpha\rho^2(0,0)F(g\mu_B/k)^{1/2}\sqrt{H}\ . \tag{18}$$

The last term in Eq. (18) gives a positive magnetoresistance proportional to $\sqrt{H}$ and independent of T. The $\sqrt{T}$ temperature dependence in the second term is always negative since $F \leq 1$.

Using a localization model, Kawabata[15] has predicted a negative magnetoresistance contribution given by

$$\frac{\rho(H,T)-\rho(0,T)}{\rho(0,0)}\equiv\frac{\Delta\rho}{\rho(0,0)}=-0.918\rho(0,0)H^{1/2} \quad \text{for } H \gg H_c \tag{19}$$

where $\rho(0,0)$ is given in Ω cm and H in kOe. Here $4eH_c/\hbar c=(D\tau_{\rm in})^{-1}$, where $\tau_{\rm in}$ is the inelastic scattering time. Estimates of $\tau_{\rm in}$ for our Si:P samples indicate that H_c is small compared to the fields used so that Eq. (19) applies.

In general, both the positive and negative magnetoresistance contributions from Eq. (18) and (19) should be present. If we assume that the separate contributions are additive, the overall magnetoresistance at large fields becomes

$$\frac{\Delta\rho}{\rho(0,0)}=\left[-0.918\rho(0,0) +0.77\alpha\rho(0,0)F\left[\frac{g\mu_B}{\kappa}\right]^{1/2}\right]\sqrt{H} -\alpha\rho(0,0)(\tfrac{4}{3}-F)\sqrt{T} \equiv(A_l+A_c)\sqrt{H}-B\sqrt{T}\ . \tag{20}$$

Since A_c is proportional to $[\rho(0,0)]^{3/2}$ we expect it to dominate near the transition.

The important features of Eq. (20) are demonstrated by Fig. 8, which shows $\rho(H,T)$ plotted against $\sqrt{H}$ at four temperatures for a sample with $\sigma(0)=2\sigma_M$. The solid lines are best fits to the data and show the $\sqrt{H}$ dependence above 300 Oe. The slopes for the four temperatures are nearly the same,

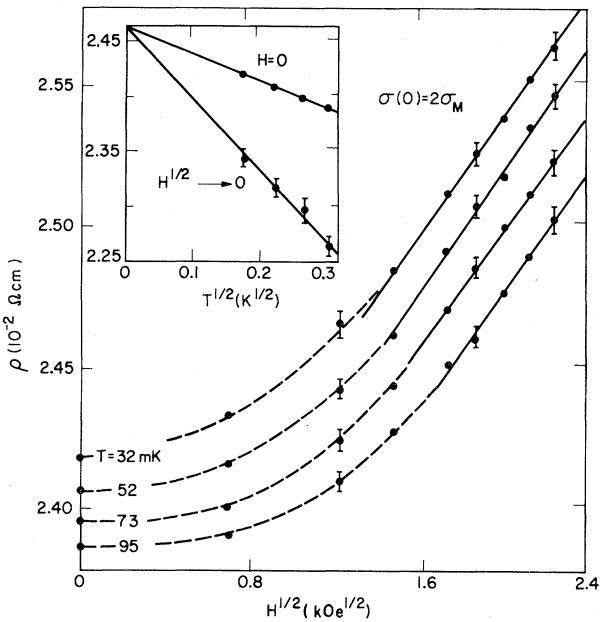

FIG. 8. ρ vs $H^{1/2}$ at four temperatures for a sample with $\sigma(0)=2\sigma_M$. At high fields ρ is proportional to $H^{1/2}$ with a slope independent of T, in agreement with Eq. (18). The intercepts of the solid lines, as well as ρ measured in zero field, are proportional to $T^{1/2}$, as shown in the inset.

in agreement with theory. The extensions of these straight lines to $\sqrt{H}\to 0$ provide values of ρ which should be linear in $\sqrt{T}$ as shown by Eq. (20). This plot is shown in the inset to Fig. 8. At $H=0$ the resistivity becomes

$$\rho(0,T)=\rho(0,0)-\alpha\rho^2(0,0)(\tfrac{4}{3}-\lambda F)\sqrt{T}\ , \qquad (21)$$

and this $\sqrt{T}$ dependence is also shown in the inset, where both curves are constrained to go through the same value of $\rho(0,0)$. From the average of the slopes of the solid lines in Fig. 8 we can obtain an experimental value for $A\equiv A_l+A_c$ in Eq. (20). We get[28] $A=0.044\pm0.004$ kOe$^{-1/2}$. From the fit in the inset we get $B=0.26\pm0.06$ K$^{-1/2}$. The theoretical evaluations of A_c and A_l are uncertain for this sample both because of the unknown scattering rates that enter F and because the sample has a dimensionless diffusion constant $m_eD/\hbar=0.4$, rather than $m_eD/\hbar\gg 1$ as assumed theoretically. However, we can make a less ambiguous comparison of theory and experiment by assuming Eq. (19) for A_l and considering the ratio B/A_c, in which αF cancels. Theoretically $B/A_c=1.3(k/g\mu_B)^{1/2}=3.5$ (kOe/K)$^{1/2}$ for $g=2$, independent of other sample parameters. Combining $A_{\rm exp}$ and Eq. (19) for A_l, we find $B/A_c=0.26/(0.044+0.023)=4\pm1(kOe/K)^{1/2}$, in agreement with theory.

Similar qualitative features are found in the magnetoresistance data of Ootuka *et al.*[29] for Ge:Sb. Their sample has a donor concentration of $\tilde{n}=0.33$, well above $\tilde{n}_c=0.155$. We have replotted their data for 10, 20, 30, and 40 mK in Fig. 9. To separate the data for the four temperatures we have plotted

$$[\rho(H,T)-\rho(0,T)]/\rho(0,T)\equiv\Delta\rho/\rho\ ,$$

against $\sqrt{H}$ rather than $\rho(H,T)$ vs $\sqrt{H}$. The solid lines again show that the magnetoresistance is proportional to $\sqrt{H}$ with a slope independent of temperature. The inset of Fig. 9 shows that the intercepts found by extending the straight line to $\sqrt{H}\to 0$ are linear in $\sqrt{T}$, as are the measured values for $H=0$. Analyzing this data in the same manner as the Si:P data of Fig. 8 we obtain $B/A_c=0.8$ (kOe/K)$^{1/2}$ as compared to the theoretical value of 3.5 (kOe/K)$^{1/2}$.

In principle, a better test of the theory embodied in Eq. (20) requires samples with $m_lD/\hbar\gg 1$. Figure 10 shows data for our most metallic Si:P sample, having $\sigma(0)=11\sigma_M$ and $m_lD/\hbar\sim 2$. For this donor concentration $|A_l|$ and A_c are nearly equal, as indicated by the very small values of $\Delta\rho/\rho(0,0)$. For low fields the magnetoresistance is negative. For $H>5$ kOe the Coulomb interaction term dominates and we find positive magnetoresistance proportional to $H^{1/2}$ as shown in Fig. 10. In zero field this sample also exhibits a negative temperature correction to $\sigma(0)$ proportional to $T^{1/2}$ as previously discussed.[27] This $T^{1/2}$ dependence is also shown in Fig. 10. If we assume that the localization factor A_l given by Eq. (19) is exact, we can combine the experimental

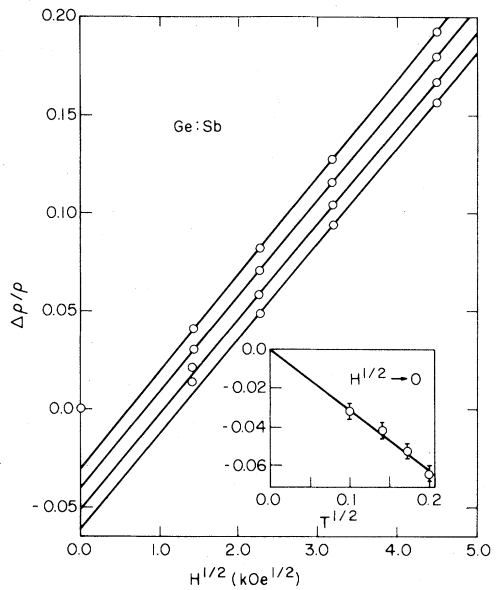

FIG. 9. $\Delta\rho/\rho$ vs $H^{1/2}$ at 10, 20, 30, and 40 mK for a Ge:Sb sample from Ref. 28. At high fields $\Delta\rho/\rho$ is proportional to $H^{1/2}$. Extrapolations of the linear region to $H^{1/2}\to 0$ yield values of $\Delta\rho/\rho$ which are proportional to $T^{1/2}$, as shown in the inset.

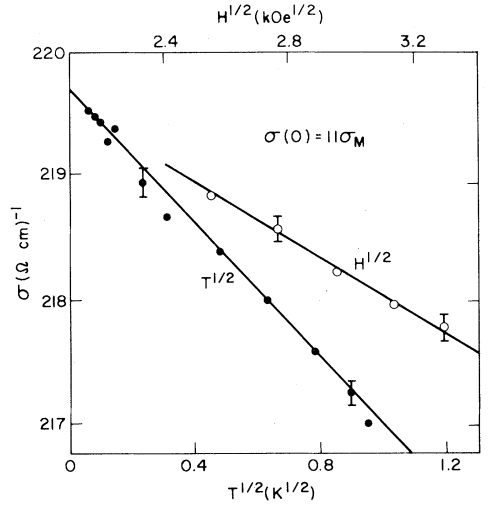

FIG. 10. σ vs $T^{1/2}$ and $H^{1/2}$, the predictions of the Coulomb interactions model, for a sample with $\sigma(0)=11\sigma_M$. The slopes of these curves yield values which can be used to calculate α and F from Eqs. (18) and (19).

values of A and m (slopes of the plots in Fig. 10) to evalute F and α separately. We find $F=0.80$ and $\alpha=11$ $(\Omega\,\mathrm{cm\,K}^{1/2})^{-1}$ compared to the theoretical values of $F=0.84$ and $\alpha=1.2$ $(\Omega\,\mathrm{cm\,K}^{1/2})^{-1}$. This discrepancy in α is also evident in the temperature correction to $\sigma(0)$ for the series of metallic samples shown in Fig. 7 where we find that the experimental values of m exceed the theoretical values by a factor of ~ 7 if corrections for the valley participation in the screening are not included.[12]

Using the experimental values of α and F, which were derived from the *slopes* of the graphs in Fig. 10, we have calculated the *amplitude* of $\Delta\rho/\rho$. Curve I in Fig. 11 is calculated using these experimental values and Eq. (17). Curve II is the localization prediction, Eq. (19), and curve III is the sum of I and II. We see that curve III is reasonably close to the experimental values, considering that it is found by taking the sum of two, large and nearly equal but opposite, effects. In other words, relatively small changes in the values of curves I and/or II will have a large influence on curve III, since we are in the regime where $|A_I| \sim A_c$. This makes precise tests of the theories difficult. Unfortunately, this is also the conductivity region $(m_I D/\hbar \gg 1)$ where we expect the theories to apply.

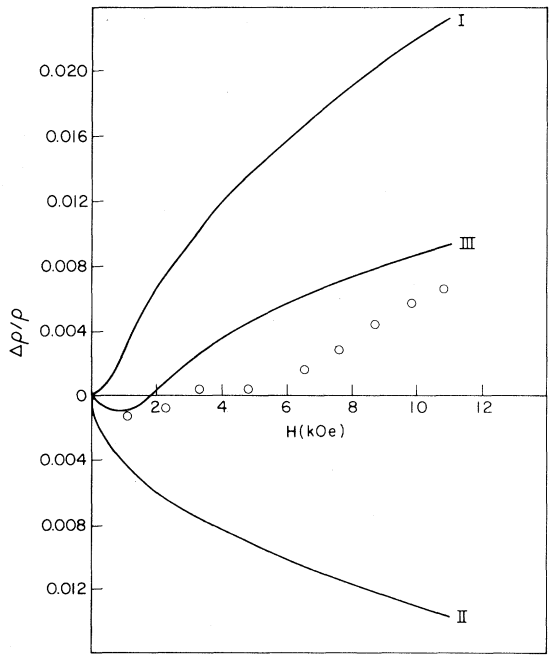

FIG. 11. Interactions theory, Eq. (18), gives curve I while localization calculations, Eq. (19), give curve II. The sum is shown in curve III, producing negative and then positive magnetoresistance as a function of H in qualitative agreement with the data.

A compensated sample of n-type Si:As:B, $K\sim 20\%$, with net carrier density 7.5×10^{18} cm^{-3} determined from Hall data at low T, still shows the large influence of Coulomb effects. Although the compensation increases the ratio of scattering centers to effective charge carriers, the magnetoresistance remains $+H^{1/2}$ as shown in Fig. 12 for $T=50$ mK and fields up to 50 kOe. This sample does, however, provide a vivid demonstration of the effect of large H on $\sigma(T)$. If $F\geq\frac{2}{3}$, then $\sigma(T)$ changes sign because of the difference between the $(\frac{4}{3}-2F)T^{1/2}$ and $(\frac{4}{3}-F)T^{1/2}$ terms in Eqs. (13) and (16), respectively. We plot $\Delta\sigma/\sigma$ vs $T^{1/2}$ for both $H=0$ and $H=50$ kOe in Fig. 13 and note the simple physical meaning of complicated equations.

Magnetoresistance measurements[45–47] of doped semiconductors at higher T show numerous instances of negative $\Delta\rho$ at low field and positive $\Delta\rho$ at high field, similar to what we have discussed here. The mechanisms described above may be responsible for some of these cases.

Very close to n_c the interaction term should dominate the localization term and we should find positive $\Delta\rho$ even at small fields. However, one should be careful in applying either Eq. (18) or Eq. (19) for samples very close to the transition. Both calculations are done in the weak scattering limit, $m_I D/\hbar \gg 1$, and near the transition this condition is not satisfied. We have previously reported[27] a large positive magnetoresistance for a sample with $\sigma(0,0)=0.16\sigma_M$. Although $\Delta\rho/\rho(0,0)$ is proportional to $\sqrt{H}$ at high fields the precise shape of the $\Delta\rho/\rho(0,0)$ vs H curve does not agree with Eq. (18).

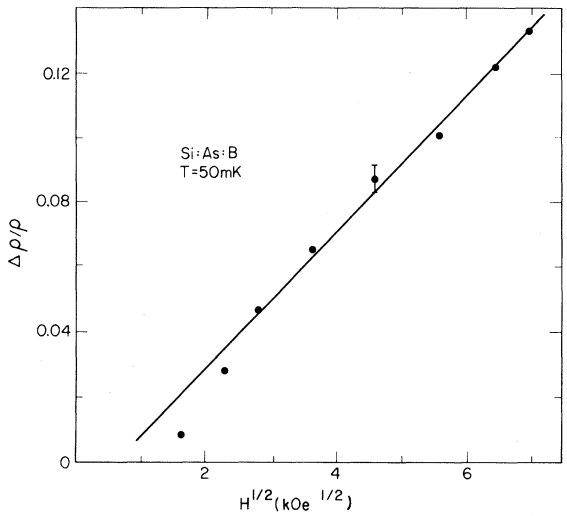

FIG. 12. Magnetoresistance of compensated Si:As:B $(K\sim 20\%)$ vs $H^{1/2}$ up to 50 kOe. The interaction effect of $+H^{1/2}$ at high field still dominates.

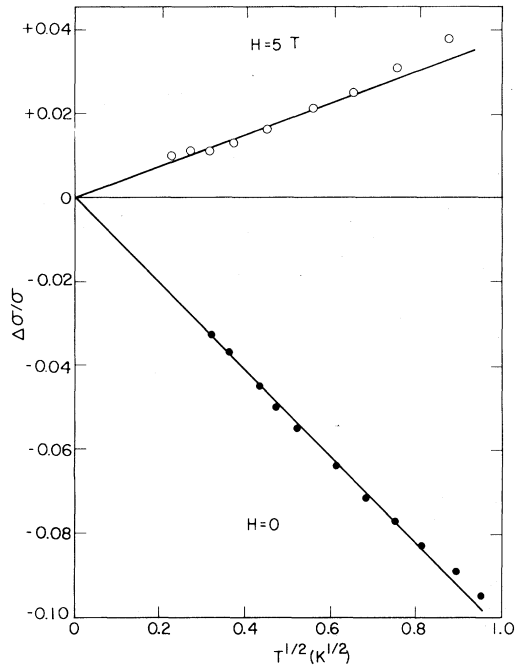

FIG. 13. Switch in sign of $T^{1/2}$ dependence of σ with application of large magnetic field H [compare Eqs. (13) and (16)].

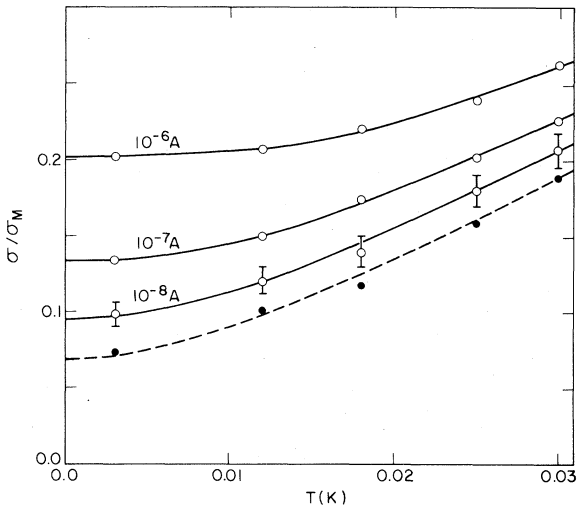

FIG. 14. σ/σ_M vs T at three current levels for a sample very close to n_c. The dotted line is the extrapolation to zero electric field. Extrapolation to both zero E and T yields $\sigma(0)/\sigma_M=0.07$, so that n is too close to n_c to give a reliable value of n/n_c-1 within our uncertainty in determining n.

D. Electric field effects

For samples with donor concentrations just below n_c we have previously shown[30] that the electric field dependence of the dc resistivity suggests that the electronic transport proceeds by hopping. The temperature and electric field dependence of the resistivity for samples with barely localized electrons takes the form

$$\rho(T,E)\propto\rho(T)\exp(eEL/k_BT)\ ,$$

where E is the electric field and L is a characteristic length. A resistivity which varies exponentially with E/T is characteristic of hopping[16,17]; however, the behavior of the $\rho(T)$ term does not unequivocally support either fixed range hopping or variable range hopping as the dominant mechanism. For transport dominated by fixed range hopping we expect the form $\ln\rho(T)\propto 1/T$, while for phonon-activated variable range hopping the form is[1] $\ln(\rho/\rho_0)=(T/T_0)^{-1/4}$. Neither form fits over an extended temperature range.[30]

For samples with donor concentrations above n_c there is also an electric field which is not related to simple lattice heating. Figure 14 shows σ/σ_M plotted against T for three different current levels. The lowest current level of 10^{-8} ampere corresponds to a power input of only $\sim 10^{-15}$ W. It is evident that over the entire T range in Fig. 14 the value of σ is tending to a nonzero saturation value as the electric field is reduced. The dotted line represents the $E\rightarrow 0$ extrapolated value of $\sigma(T)$, based on the data. Figure 15 shows one possible method of extrapolating the finite field data. We have plotted the measured values of σ/σ_M at finite T and E as a function of $E^{1/2}$ for T values of 3, 25, and 41 mK. We see that in this low-field limit σ is consistent with the form $E^{1/2}$. At higher values of E the effect of electronic heating is masked by lattice heating. Using the values of σ extrapolated to zero field, we then plot σ against T. This sample is very close to n_c and has a positive T correction to $\sigma(0)$. Extrapolating to zero E and zero T we find $\sigma/\sigma_M=0.07$ for this sample, as indicated by the arrow in Fig. 15.

The effect of E is reduced for both higher temperatures and higher donor concentrations. Figure 16 shows σ/σ_M plotted against $E^{1/2}$ for two samples above σ_M. For the $2\sigma_M$ sample there is a modest electric field effect (note the expanded vertical scale) which is largest at low T. This sample has a temperature correction to $\sigma(0)$ given by Eq. (7) with $\beta\sim\frac{1}{2}$ and positive m. The $11\sigma_M$ sample has a negligible electric field effect and has $\beta\sim\frac{1}{2}$ with negative m.

E. Metallic samples near the transition

We have already seen that the effects on σ of temperature, electric field, and magnetic field are

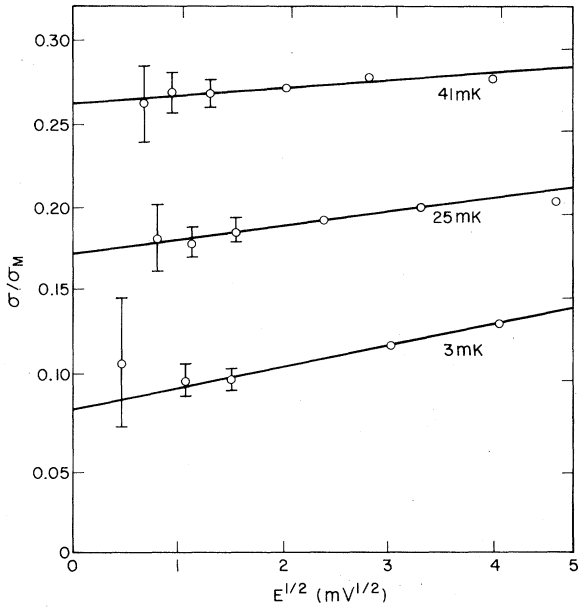

FIG. 15. σ/σ_M vs $E^{1/2}$ at three values of T for the sample shown in Fig. 14. Arrow shows the extrapolation to zero E and T.

greatest near n_c. Unfortunately, this is also the region where the theoretical approximations are not satisfied and where experimental rounding occurs.

Over a wide range of conductivities [$\sigma(0)/\sigma_M \sim 10^{-3}$ to 10^3] we find that Eq. (7) adequately describes $\sigma(T)$. For samples with $\sigma(0)/\sigma_M > 1$ we find the best fit is $\beta \sim \frac{1}{2}$ with m changing from negative to positive as $n \to n_c$. However, for $\sigma(0)/\sigma_M \lesssim 0.2$ we find $\beta \sim 2$ with positive m. Figure 17 is a plot of $\log[\sigma - \sigma(0)]$ against $\log T$. Here the values of $\sigma(0)$ were chosen to yield a straight line on this plot. Data for the $\sigma(0) = 0.001\sigma_M$ sample is shown before (closed circle) and after (open circle) annealing at 1030°C for 96 h. Annealing produced only minor changes in $\sigma(T)$ for this sample indicating a fairly homogeneous (or unchanged) distribution of donor impurities. The open circles near the right edge are the post anneal data for a sample which before annealing had $\sigma(0) = 0.03\sigma_M$. In this case annealing pushed the sample through the metal-insulator transition. Perhaps this sample was originally less homogeneous than the $0.001\sigma_M$ sample and metallic channels enhanced its conductivity.

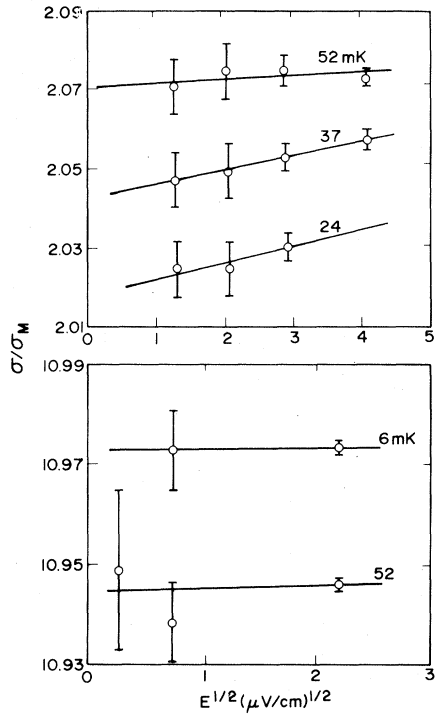

FIG. 16. σ/σ_M vs $E^{1/2}$ for samples with (a) $\sigma(0) = 2\sigma_M$ and (b) $\sigma(0) = 11\sigma_M$. Significant electric field dependence is only found for samples very close to the transition and does not present a problem in the more metallic regime.

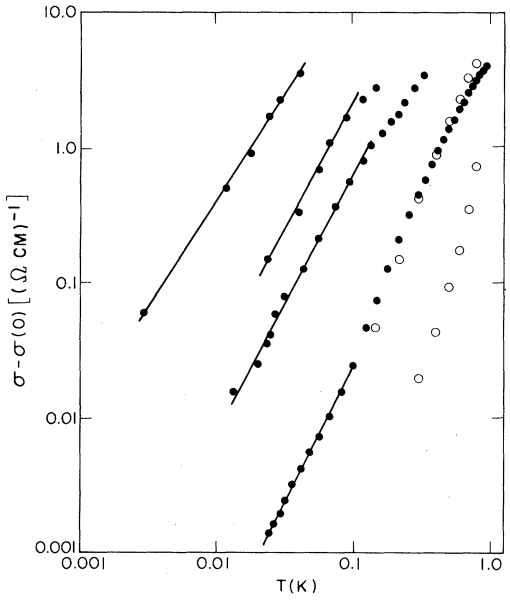

FIG. 17. Logarithmic plot of $\sigma - \sigma(0)$ vs T for samples very close to the transition. The solid lines correspond to $\beta \sim 2$. The values of $\sigma(0)$ are shown in Fig. 18; the values of n are all within 1% of n_c and thus we cannot specify values of $n/n - 1$ because of our uncertainty in n. The $\sigma(0) = 0.001\sigma_M$ sample shows data before (closed circles) and after annealing (open circles). Data on the right side are the post annealing results for an insulating sample showing exponential T dependence, where $\sigma(0) = 0$.

In Fig. 18 we plot the experimental values of β against $\log\sigma(0)/\sigma_M$. We see that $\beta\sim\frac{1}{2}$ for $\sigma(0)/\sigma_M > 1$ and $\beta\sim 2$ for $\sigma(0)/\sigma_M \lesssim 0.2$, a result also seen in stress-tuned samples. It is not clear if this effect is related to finite frequency, Shottky barriers, surface conduction, or a nonrandom impurity distribution. We are not aware, however, of any theory which predicts a bulk conductivity given by $\sigma(T)=\sigma(0)+mT^2$ near the transition.

Mooij[48] has shown that as a general rule metallic alloys which are highly disordered, and hence have large resistivity, exhibit a small (often negative) temperature coefficient of resistivity (TCR). Alloys with resistivities less than $\sim 150\ \mu\Omega$ cm tend to have positive TCR, while those with greater resistivities have negative TCR. This upper limit of resistivity is the order of $1/\sigma_M$ for these systems, which is approximately a statement that $k_F l \gtrsim 1$. Jonson and Girvin[49] have proposed that the Mooij correlation between TCR and ρ is the result of phonon-assisted hopping of electrons from one site to another. They argue that this occurs even before the onset of Anderson localization and limits the value of ρ for these high resistivity alloys. In Fig. 19 we have made a Mooij-type plot of several samples at different temperatures. On the ordinate we plot $(T^{1/2}/\rho)d\rho/dT$ rather than $(1/\rho)d\rho/dT$ so that the plots at different temperatures are conveniently spaced in the graph. We see that for relatively high T the plots show the characteristics of phonon effects, a diminishing (and finally negative) TCR with increasing ρ. The plots of low T are quite different. At $T=0.04$ K we see a large increase of TCR with ρ. We have already interpreted this temperature dependence of the resistivity as arising from Coulomb interactions, rather than a phonon effect.

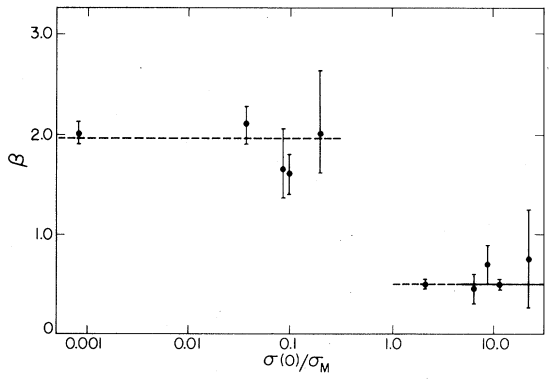

FIG. 18. Experimental values of β vs $\log[\sigma(0)/\sigma_M]$. Above $\sigma(0)/\sigma_M\sim 1$ we find $\beta\sim\frac{1}{2}$. Closer to the transition β is ~ 2. Stress results (Ref. 24) also find $\beta\sim 2$ for $\sigma(0)/\sigma_M \lesssim 0.2$.

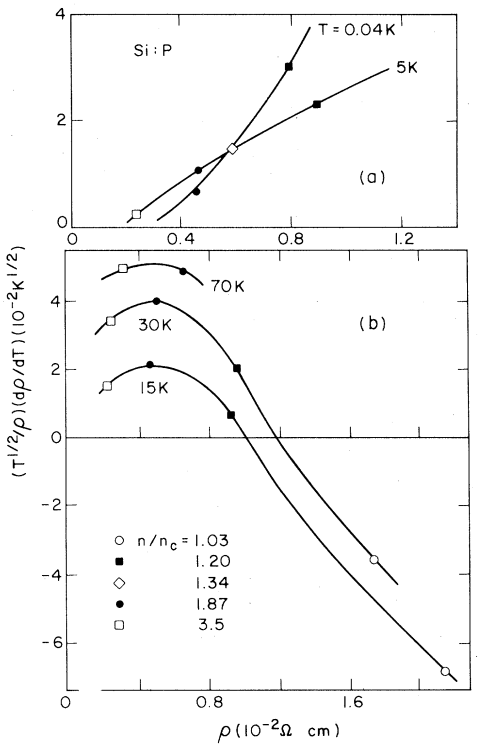

FIG. 19. $(T^{1/2}/\rho)d\rho/dT$ vs ρ for several samples and temperatures. At low T (a), where phonon effects are negligible, the data deviate from a Mooij-type dependence [linear region of (b)].

Since the number of phonons decrease as T^3 it is not surprising that phonon effects are minimal at 0.04 K and that the Mooij correlation breaks down.

In conclusion, we have measured the conductivity of Si:P samples as a function of donor concentration, temperature, magnetic field, electric field, and uniaxial stress. The dielectric constant was also measured for various donor concentrations. We find no evidence for a minimum metallic conductivity near the metal-insulator transition. We also find disagreement with the quantitative estimates of the scaling theories of localization. The temperature and magnetic field dependence of σ as well as the sharpness of the transitions of σ and χ when plotted against n suggest that Coulomb interaction effects are important in this disordered system.

Note added in proof. For a refined analysis of the conductivity very near n_c, see Ref. 51.

ACKNOWLEDGMENTS

We would like to thank L. P. Adda for annealing a series of samples and R. E. Miller and J. B. Mock for help in sample preparation.

APPENDIX

In order to quantitatively analyze our $\sigma(0)$ results for samples outside the region where localization theories are thought to be valid $(n/n_c - 1 > 0.05)$, we have calculated the conductivity for normal metallic behavior. The normal zero-temperature conductivity σ_B of a Fermi gas of electrons at the same density distributed in the six conduction-band valleys and scattered by the ionized impurities is shown as the dashed line in Fig. 20. As can be seen, there is a large "precursive" region extending up to $n/n_c \sim 2$ for which $\sigma(0)$ is suppressed. The calculation excludes intervalley and multiple scattering and is done within the Born approximation using Thomas-Fermi screening. Further, because of the large mass anisotropy, it has been assumed that each electron is effectively screened by electrons in only two valleys—its own and the coaxial valley. This is because differently oriented ellipsoidal Fermi seas have very different Fermi momenta (which determines the wave-vector dependent dielectric constant and hence the screening) in different directions. Though strictly time only for infinite mass anisotropy, the greater weight given to large momentum transfer in a resistivity calculation makes the approximation reasonable for finite, large anisotropy as well. The result, which can be obtained by generalizing the calculation for the single-valley case,[50] is

$$\sigma_B = \frac{e^2}{2\pi\hbar a^*} \frac{(k_F a^*)^3}{\ln[1+1/\gamma] - 1/(1+\gamma)} . \qquad \text{(A1)}$$

Here $k_F = (\pi^2 n/2)^{1/3}$ is an average Fermi momentum, $a^* = \epsilon\hbar/m^* e^2$ is the Bohr radius for an averaged effective mass m^*, ϵ is the Si dielectric constant, and $\gamma = \tilde{v}/\pi k_F a^*$, where $\tilde{v}$ is the number of valleys screening each electron ($\tilde{v}=2$ for Si). Except for the crucial dependence of screening effect of mass anisotropy has been approximated by appropriately averaged quantities. Such a calculation is expected to be valid for $n \gg n_c$, but below where intervalley and multiple scattering becomes important, to a level ~ 20—30%.

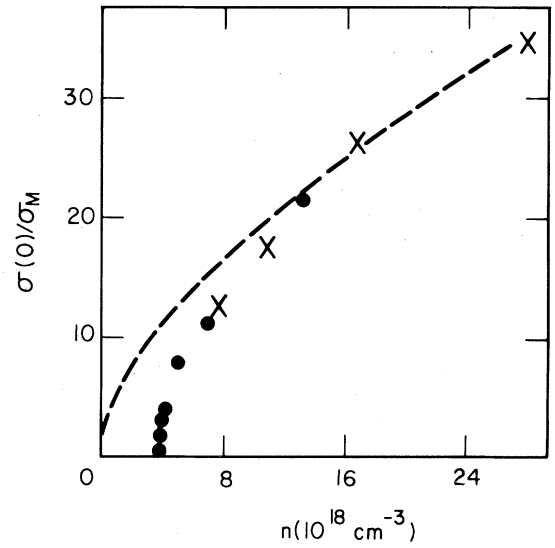

FIG. 20. Plot of σ vs n for Si:P. The dashed line is calculated using the Born approximation. There are significant deviations of the data from normal metallic conduction even far above the transition.

*Present address: James Franck Institute, The University of Chicago, Chicago, IL 60637.

†Present address: Muhlenberg College, Allentown, PA 18104.

[1]N. F. Mott, *Metal-Insulator Transitions* (Taylor and Francis, London, 1974); N. F. Mott and E. A. Davis, *Electronic Processes in Non-Crystalline Materials* (Oxford University Press, Oxford, 1979). The scaling of n_c with a_B has been documented by P. P. Edwards and M. J. Sienko, Phys. Rev. B 17, 2575 (1978).

[2]*The Metal-Insulator Transition in Disordered Systems*, edited by L. R. Friedman and D. P. Tunstall (SUSSP, Edinburgh, 1978).

[3]P. W. Anderson, Phys. Rev. 102, 1008 (1958).

[4]N. F. Mott, Philos. Mag. B 37, 377 (1978).

[5]E. Abrahams, P. W. Anderson, D. C. Licciardello, and T. V. Ramakrishnan, Phys. Rev. Lett. 42, 673 (1979); Y. Imry, *ibid.* 44, 469 (1980); C. Wegner, Z. Phys. B 25, 327 (1976); D. Vollhardt and P. Wölfle, Phys. Rev. Lett. 45, 842 (1980); A. McKinnon and B. Kramer, *ibid.* 47, 1546 (1981); D. Belitz, A. Gold, and W. Götze, Z. Phys. B 44, 273 (1981).

[6]W. Götze, J. Phys. C 12, 1279 (1979).

[7]N. F. Mott, Philos. Mag. 26, 1015 (1972); N. F. Mott, *ibid.* B 44, 265 (1981); N. F. Mott and M. Kaveh, J. Phys. C 14, L177 (1981); 14, L183 (1981); 15, L707 (1982); N. F. Mott, Proc. R. Soc. London Ser. A 382, 1 (1982).

[8]A. F. Ioffe and A. R. Regel, Prog. Semicond. 4, 37 (1960).

[9]B. L. Altshuler and A. G. Aronov, Zh. Eksp. Teor. Fiz. 77, 2028 (1979) [Sov. Phys.—JETP 50, 968 (1979)]; Zh. Eksp. Teor. Fiz. Pis'ma Red. 27, 700 (1978) [JETP Lett. 27, 662 (1978)]; Solid State Commun. 36, 115 (1979).

[10]B. L. Altshuler, A. G. Aronov, and P. A. Lee, Phys. Rev. Lett. 44, 1288 (1980); B. L. Altshuler, D. Khmelnitzkii, A. I. Larkin, and P. A. Lee, Phys. Rev. B 22,

5142 (1980). B. L. Altshuler and A. G. Aronov, Solid State Commun. 38, 11 (1981).
[11]P. A. Lee and T. V. Ramakrishnan, Phys. Rev. B 26, 4009 (1982).
[12]R. N. Bhatt and P. A. Lee (unpublished).
[13]P. W. Anderson (private communication).
[14]W. L. McMillan, Phys. Rev. B 24, 2739 (1981); B. W. Dodson, W. L. McMillan, J. M. Mochel, and R. C. Dynes, Phys. Rev. Lett. 46, 46 (1981).
[15]A. Kawabata, Solid State Commun. 34, 431 (1980); J. Phys. Soc. Jpn. 49, Suppl. A, 375 (1980).
[16]M. Pollak and I. Riess, J. Phys. C 9, 2339 (1976).
[17]R. M. Hill, Philos. Mag. 24, 1307 (1971).
[18]B. Movaghar and G. W. Sauer, Solid State Commun. 35, 841 (1980).
[19]H. Fukuyama and K. Yosida, J. Phys. Soc. Jpn. 46, 102 (1979).
[20]M. H. Alexander and D. F. Holcomb, Rev. Mod. Phys. 40, 815 (1968).
[21]H. Fritzsche, in Ref. 2.
[22]T. F. Rosenbaum, K. Andres, G. A. Thomas, and P. A. Lee, Phys. Rev. Lett. 46, 568 (1981).
[23]G. A. Thomas, A. Kawabata, Y. Ootuka, S. Katsumoto, S. Kobayashi, and W. Sasaki, Phys. Rev. B 24, 4886 (1981); C. Yamanouchi, K. Mizuguchi, and W. Sasaki, J. Phys. Soc. Jpn. 22, 859 (1967).
[24]T. F. Rosenbaum, K. Andres, G. A. Thomas, and R. N. Bhatt, Phys. Rev. Lett. 45, 1723 (1980); G. A. Thomas, T. F. Rosenbaum, and R. N. Bhatt, *ibid.* 46, 1435 (1981).
[25]M. A. Paalanen, T. F. Rosenbaum, G. A. Thomas, and R. N. Bhatt, Phys. Rev. Lett. 48, 1284 (1982); R. N. Bhatt, Phys. Rev. B 24, 3630 (1981); 26, 1082 (1982).
[26]G. A. Thomas, Y. Ootuka, S. Katsumoto, S. Kobayashi, and W. Sasaki, Phys. Rev. B 25, 4288 (1982).
[27]G. A. Thomas, Y. Ootuka, S. Katsumoto, S. Kobayashi, and W. Sasaki, Phys. Rev. B 26, 2113 (1982).
[28]T. F. Rosenbaum, R. F. Milligan, G. A. Thomas, P. A. Lee, T. V. Ramakrishnan, R. N. Bhatt, K. DeConde, H. Hess, and T. Perry, Phys. Rev. Lett 47, 1758 (1981).
[29]Y. Ootuka, S. Kobayashi, S. Ikehata, W. Sasaki, and J. Kondo, Solid State Commun. 30, 169 (1979).
[30]T. F. Rosenbaum, K. Andres, and G. A. Thomas, Solid State Commun. 33, 663 (1980); H. F. Hess, K. DeConde, T. F. Rosenbaum, and G. A. Thomas, Phys. Rev. B 25, 5578 (1982).
[31]K. Andres, R. N. Bhatt, P. Goalwin, T. M. Rice, and R. E. Walstedt, Phys. Rev. B 24, 244 (1981); R. N. Bhatt and T. M. Rice, Philos. Mag. B 42, 859 (1980).
[32]R. N. Bhatt and P. A. Lee, J. Appl. Phys. 52, 1703 (1981); Phys. Rev. Lett. 48, 344 (1982); R. N. Bhatt, *ibid.* 48, 707 (1982).
[33]T. G. Castner, N. K. Lee, G. S. Cieloszyk, and G. L. Salinger, Phys. Rev. Lett. 34, 1627 (1975); P. Townsend, J. Phys. C 11, 1481 (1978); H. S. Tan and T. G. Castner, Phys. Rev. B 23, 3983 (1982); T. G. Castner, J. Low Temp. Phys. 38, 447 (1980); for values of ϵ_0 in Si and Ge, see Faulkner, Phys. Rev. 184, 713 (1969).
[34]H. F. Hess, K. DeConde, T. F. Rosenbaum, and G. A. Thomas, Phys. Rev. B 25, 5585 (1982).
[35]G. A. Thomas, M. Capizzi, and F. DeRosa, Philos. Mag. B 42, 913 (1980).
[36]M. Capizzi, G. A. Thomas, F. DeRosa, R. N. Bhatt, and T. M. Rice, Phys. Rev. Lett. 44, 1019 (1980).
[37]M. Capizzi, G. A. Thomas, F. DeRosa, R. N. Bhatt, and T. M. Rice, Solid State Commun. 31, 611 (1979); G. A. Thomas, M. Capizzi, F. DeRosa, R. N. Bhatt, and T. M. Rice, Phys. Rev. B 23, 5472 (1981).
[38]Y. Ootuka, F. Komori, Y. Monden, S. Kobayashi, and W. Sasaki, Solid State Commun. 33, 793 (1980); 36, 827 (1980).
[39]D. E. Schafer, F. Wudl, G. A. Thomas, J. P. Ferraris, and D. O. Cowan, Solid State Commun. 14, 347 (1974).
[40]K. Andres, Cryogenics 18, 473 (1978).
[41]F. Mousty, P. Ostoja, and L. Passari, J. Appl. Phys. 45, 4576 (1974).
[42]Y. Imry, Y. Gefen and D. J. Bergman, in Vol. 39 of *Springer Series in Solid State Physics* (Springer, New York, 1982), p. 138.
[43]R. C. Dynes and J. P. Garno, Phys. Rev. Lett. 46, 137 (1981).
[44]See, for example, C. Kittel, *Introduction To Solid State Physics* (Wiley, New York, 1976).
[45]O. N. Tufte and E. L. Stelzer, Phys. Rev. A 139, 265 (1965).
[46]H. Roth, W. D. Straub, and W. Bernard, Phys. Rev. Lett. 11, 328 (1963).
[47]Y. Ootuka, S. Ikehata, S. Kobayashi, and W. Sasaki, Solid State Commun. 20, 441 (1976).
[48]J. H. Mooij, Phys. Status Solidi A 17, 521 (1973).
[49]M. Jonson and S. M. Girvin, Phys. Rev. Lett. 43, 1447 (1979).
[50]See, e.g., N. F. Mott, Proc. Cambridge Philos. Soc. 32, 281 (1936) or J. B. Krieger and S. Strauss, Phys. Rev. 169, 674 (1968).
[51]G. A. Thomas, M. Paalanen, and T. F. Rosenbaum, Phys. Rev. B 27, 3897 (1983).